



# In silico Characterization of a Hypothetical Protein (PBJ89160.1) from *Neisseria meningitidis* Exhibits a New Insight on Nutritional Virulence and Molecular Docking to Uncover a Therapeutic Target

Evolutionary Bioinformatics  
Volume 20: 1–16  
© The Author(s) 2024  
Article reuse guidelines:  
sagepub.com/journals-permissions  
DOI: 10.1177/11769343241298307



Israt Jahan Asha, Shipan Das Gupta, Md. Murad Hossain ,  
Md. Nur Islam, Nurun Nahar Akter, Mohammed Mafizul Islam,  
Shuvo Chandra Das and Dharendra Nath Barman 

Department of Biotechnology and Genetic Engineering, Noakhali Science and Technology University, Noakhali, Bangladesh

## ABSTRACT

**OBJECTIVE:** *Neisseria meningitidis* is an encapsulated, diplococcus, kidney bean-shaped bacteria that causes bacterial meningitis. Our study hopes to advance our understanding of disease progression, the spread frequency of the bacteria in people, and the interactions between the bacteria and human body by identifying a functional protein, potentially serving as a target for meningococcal medicine in the future.

**METHODS:** A hypothetical protein HP (PBJ89160.1) from *N. meningitidis* was employed in this study for extensive structural and functional characterization. In the predictive functional role of HP, several constitutive bioinformatics approaches are applied, such as prediction of physiological properties, domain and motif family function, secondary and tertiary structure prediction, energy minimization, quality validation, docking, and ADMET analysis. To create the protein's three-dimensional (3D) structure, a template protein (PDB\_ID: 3GXA) is used with 99% sequence identity by homology modeling technique with the HHpred server. To mitigate the pathogenicity associated with the HP function, it was docked with the natural ligand methionine and five other drug compounds like Verapamil, Loperamide, Thioridazine, Chlorpromazine, and Auranofine.

**RESULTS:** The protein is predicted to be acidic, soluble and hydrophilic by physicochemical properties analysis. Subcellular localization analysis demonstrated the protein to be periplasmic. The HP has an ATP-binding cassette transporter (also known as ABC transporter) involved in uptake of methionine (MetQ) that creates nutritional virulence in host. Energy minimization, multiple quality assessments, and validation value determination led to the conclusion that the HP model had a workable and acceptable quality. Following ADMET analysis and binding affinity assessments from the docking studies, Loperamide emerged as the most promising therapeutic compound, effectively inhibiting the ATP transporter activity of the HP.

**CONCLUSION:** Comparative genomic analysis revealed that this protein is specific to *N. meningitidis* and has no homologs in human proteins, thereby identifying it as a potential target for therapeutic intervention.

**KEYWORDS:** ATP-binding cassette transporter, ABC transporter superfamily, MET-Q, hypothetical protein, nutritional virulence

**RECEIVED:** May 9, 2024. **ACCEPTED:** October 22, 2024.

**TYPE:** Original Research

**FUNDING:** The author(s) received no financial support for the research, authorship, and/or publication of this article.

**DECLARATION OF CONFLICTING INTERESTS:** The author(s) declared no potential conflicts of interest with respect to the research, authorship, and/or publication of this article.

**CORRESPONDING AUTHOR:** Dharendra Nath Barman, Department of Biotechnology and Genetic Engineering, Noakhali Science and Technology University, Noakhali 3814, Bangladesh. Emails: dhiren.bge@nstu.edu.bd; dhirenbcm@yahoo.com

## Introduction

By colonizing upper respiratory mucosal surfaces, the gram-negative facultative pathogenic bacteria *Neisseria meningitidis* of the pseudomonadota group can cause invasive meningococcal disease.<sup>1</sup> *N. meningitidis* colonizes the nasopharynx, crossing mucosal host defenses to bind to human epithelial cells. It can multiply rapidly, allowing it to enter the bloodstream and cause sepsis, and cause meningeal, pericardial, and joint infections.<sup>2</sup> Meningitis is caused by bacteria that can proliferate in cerebrospinal fluid due to crossing the blood-brain barrier.

While healthcare professionals have expressed worry about the susceptibility of meningococci to penicillin and other antibiotics employed in managing meningococcal disease, it has been widely recognized that penicillin remains the preferred antibiotic

for treating meningococcal infections.<sup>3</sup> Contrarily, there have recently been numerous reports of penicillin-resistant meningococci from places including Spain,<sup>4</sup> Italy,<sup>5</sup> Greece,<sup>6</sup> the United Kingdom,<sup>7</sup> the United States,<sup>8</sup> and Israel.<sup>9,10</sup> Among the main bacterial causes of meningitis, *N. meningitidis* is distinct because it can spread endemic (sporadic) illness as well as epidemic meningitis. Major meningococcal disease outbreaks still occur often in the African meningitis belt, such as in sub-Saharan Africa.<sup>11</sup> In Sub-Saharan Africa, serogroup A *N. meningitidis* was responsible for the greatest meningococcal epidemic outbreak ever, which resulted in over 300,000 cases and 30,000 fatalities.<sup>12</sup>

Since 1980, significant serogroup B epidemics and/or outbreaks of serogroup A or C meningitis have also occurred in Europe, the United States, Canada, China, Nepal, Mongolia, New Zealand, Cuba, Brazil, Chile, Saudi Arabia, and South



Creative Commons Non Commercial CC BY-NC: This article is distributed under the terms of the Creative Commons Attribution-NonCommercial 4.0 License (<https://creativecommons.org/licenses/by-nc/4.0/>) which permits non-commercial use, reproduction and distribution of the work without further permission provided the original work is attributed as specified on the SAGE and Open Access pages (<https://us.sagepub.com/en-us/nam/open-access-at-sage>).

Africa.<sup>13–16</sup> In November 2020, the World Health Assembly approved the global roadmap to defeat meningitis, which aims to eliminate bacterial meningitis epidemics, reduce vaccine-preventable cases and deaths by 50% and 70%, respectively, decrease disability, and enhance the quality of life. Key to this initiative is the development of novel, cost-effective vaccines such as NmCV-5.<sup>17</sup>

Despite the development of vaccine like NmCV-5, the antibiotic resistance attracts the attention of researchers to consider other pharmacological targets to combat meningococcal disease. Researchers are particularly interested in studying hypothetical proteins (HP) because they lack proper functional annotations and are derived from open reading frames without any experimental evidence of translation. *N. meningitidis* strain M26503 has 2115 encoded proteins, of which 386 are yet to be characterized. These HPs belong to uncharacterized protein families and domains with unknown functions.<sup>18</sup> The recognition and characterization of HP play a crucial role in the selection of targets for drug design.<sup>19</sup> For instance, Naveed et.al (2017) annotated six HPs from human adenovirus as novel drug targets.<sup>20</sup> Therefore, we tried to address a HP (PBJ89160.1) of *N. meningitidis* using in silico approach to establish it as a new functional protein that is supposed to be a prospective therapeutic target.

Meanwhile, Bacteria often scavenge vital nutrients, such as amino acids, from their hosts to overcome the host's natural defenses and/or develop mechanisms which target important host biosynthetic pathways. This strategy, known as “nutritional virulence.”<sup>21</sup> We were concerned whether this HP has the capability to induce nutritional virulence or not. Therefore, by performing molecular docking, it is believed that this protein might play a crucial role in nutritional virulence as well as a methionine transporter in the ABC transport mechanism.

## Materials and Methods

### Sequence retrieval

In this study, we accessed the genome of *Neisseria meningitidis* CNQ34\_02465 from the database of National Center for Biotechnology Information (NCBI) (<http://www.ncbi.nlm.nih.gov>). The chosen focus was a hypothetical protein from this *N. meningitidis* strain having 287 amino acid residues (accession no. PBJ89160.1). In order to facilitate downstream investigations, the protein sequence was acquired in FASTA format. The complete workflow, the bioinformatics tools and databases have been depicted in Figure 1.

### Analysis of physicochemical properties

ProtParam tool (<http://web.expasy.org/protparam/>)<sup>22</sup> of ExPASy was used to examine the HP's physical and chemical characteristics, such as its molecular weight, extinction coefficients, aliphatic index (AI), isoelectric point (pI), and GRAVY (grand average of hydropathy).

### Subcellular localization and solubility prediction

The subcellular localization of the HP was predicted using CELLO (<http://cello.life.nctu.edu.tw/>),<sup>23</sup> PSLpred (<https://webs.iitd.edu.in/raghava/pslpred/submit.html>)<sup>24</sup> and BUSCA (<https://busca.biocomp.unibo.it/>).<sup>25</sup> To calculate the average hydrophobicity and estimate the solubility of the protein, SOSUI was employed (<http://harrier.nagahama-i-bio.ac.jp/sosui/>).<sup>26</sup> Transmembrane areas were identified via the SOSUI server. Additionally, the prediction of the protein's solubility was carried out using the Protein sol server (<http://protein-sol.manchester.ac.uk/>).<sup>27</sup>

### Function prediction by domain and motif analysis

Various tools were utilized for domain analysis, including the NCBI Conserved Domain Search Service (CD Search) (<https://www.ncbi.nlm.nih.gov/Structure/cdd/wrpsb.cgi>)<sup>28</sup> and InterProScan (<http://www.ebi.ac.uk/Tools/services/web/toolform.ebi?tool=iprscan5>).<sup>29</sup> The conserved domains of a protein sequence are detected through CD Search. RPS-BLAST (Reverse Position Specific BLAST), which compares a query sequence to position-specific score matrices derived from conserved domain alignments in the Conserved Domain Database (CDD), assesses the query sequence against these alignments. The ScanProsite (<https://prosite.expasy.org/scanprosite/>)<sup>30</sup> service was utilized to scrutinize the motif in the protein sequence.

### Pathway analysis

KEGG pathway data sets were retrieved from KEGG server<sup>31</sup> (<https://www.genome.jp/>). The KEGG pathway database is a comprehensive collection of manually curated pathway maps that depict our understanding of molecular interactions, reactions, and relationship networks across various biological processes. These include metabolism, genetic information processing, environmental information processing, cellular processes, organismal systems, human diseases, and drug development. The KEGG ID for the HP in this study is K02073.

### Protein network map

The functional association between two or more proteins that induce a biological effect can be investigated using the Search Tool for the Retrieval of Interacting Genes/Proteins (STRING) database. Accordingly, a STRING 12.0 search was conducted to identify potential functional interaction networks for the HP under study (<https://string-db.org/>).<sup>32</sup>

### Protein family and phylogenetic tree analysis

The analysis involved utilizing Protein-BLAST (BLASTp)<sup>33</sup> through NCBI. The search was performed against the

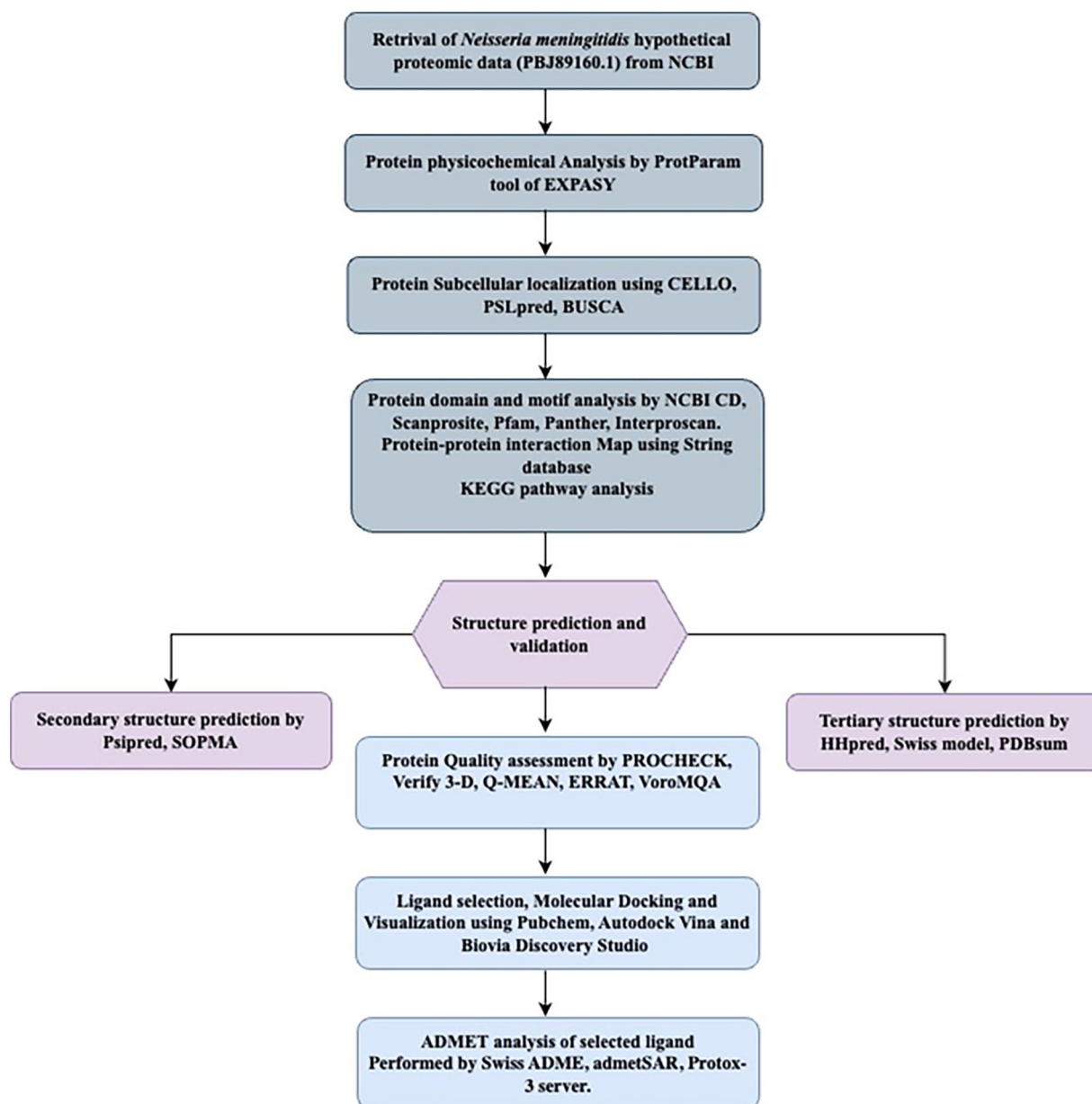


**Figure 1.** A complete workflow with used database in this study.

non-redundant database using default parameters to locate homologs of HP. This method relies on local protein sequence alignment to identify proteins with comparable functions. To align multiple sequences and construct phylogenetic trees for a limited set of chosen sequences, MEGA 11 version was employed.<sup>34</sup>

#### Secondary structure determination

The self-optimized prediction method with alignment (SOPMA)<sup>35</sup> was employed to predict the secondary structure. The outcomes from PSIPRED (<http://bioinf.cs.ucl.ac.uk/psipred/>)<sup>36</sup> and ENDscript (<http://endscript.ibcp.fr/ESPrpt/ENDscript/>)<sup>37</sup> were compared and cross-referenced with the results obtained from SOPMA.

#### Homology modeling

To predict the 3D structure of the hypothetical protein, a comparative analysis was conducted using pairwise comparison of profile hidden Markov models (HMMs) and the HHpred server. Beyond multiple alignments between the query and a set of templates selected from the search results, HHpred has the capability to generate pairwise query-template alignments. The MODELLER software can then use these alignments to generate 3D structural models.<sup>38</sup> A 3D model of the putative protein that displays 99% identity was constructed using the template protein (PDB\_ID: 3GXA-C). The structure of the 3D model was visualized using BIOVIA Discovery Studio Visualizer (version 20.1.0.19295).<sup>39</sup> To visualize the detailed protein ligand interaction, another server, PDBsum<sup>40</sup> was used.

### *Energy minimization of the model structure*

The energy minimization of predicted three-dimensional model structure from HHpred server was employed by YASARA force field minimizer.<sup>41</sup> It reduces energy consumption and provides reliable and precise 3D structure of the hypothetical protein.

### *Active site determination*

The web-based tool Computed Atlas of Surface Topography of Protein (CASTp) (<http://sts.bioengr.uic.edu/castp>)<sup>42</sup> was employed to identify the protein's active site. CASTp is instrumental in detecting, outlining, and quantifying geometric and topological features crucial for proper protein function, such as surface pockets, interior cavities, and cross channels. Additionally, it facilitates the mapping of functionally annotated residues on protein 3D structures.

### *Quality assessment*

The quality of the HP 3D structure was assessed using PROCHECK,<sup>43</sup> Verify3D (<https://servicesn.mbi.ucla.edu/Verify3D/>),<sup>44</sup> QMEAN (<https://swissmodel.expasy.org/qmean/>),<sup>45</sup> programs available on the ExPASy server of the SWISS-MODEL Workspace and ERRAT (<https://servicesn.mbi.ucla.edu/ERRAT/>).<sup>46</sup> Software from UCSF called Chimera was also used to overlay the hypothetical protein and the template structure and visualize the results.<sup>47</sup> By employing the ProSA-web server, the template and hypothetical proteins Z scores were calculated.<sup>48</sup> To enrich our validation, VoroMQA tool was used.<sup>49</sup>

### *Comparative genomics approach*

The proteome datasets of *Homo sapiens* was searched against the HP using BLASTp (<https://blast.ncbi.nlm.nih.gov/Blast.cgi?PAGE=Proteins>) to determine whether this HP, resembles any human proteins. A minimum bit score of 100 and a threshold *E*-value (expected value) of 0.005 were used to filter the hits.

### *Molecular docking analysis*

AutoDock Vina was used to perform molecular docking to predict probable receptor-substrate interactions.<sup>50</sup> Structural evidence from a previous study indicates that the template protein 3GXA (GNA1946) is an L-methionine binding lipoprotein located in the outer membrane.<sup>51</sup> Thus, methionine is a natural compound that acts as a ligand for the HP. To assess the binding affinity between the ligand and the Hypothetical Protein, as well as a template protein (3GXA) with a 3D structure modeled using HHpred and MODELER, AutoDock Vina was employed. The docking results were subsequently examined using Discovery Studio Visualizer and PyMOL 3.0 software.<sup>52</sup> To perform docking analysis, the initial step was to

prepare the hypothetical protein and ligand. For protein preparation, ligand and water molecules were removed, and polar hydrogen atoms were added to the HP using AutoDock tool. At the same time, Kollman and Gasteiger charges were differently assigned as partial charge to the receptor and ligand respectively. The protein was then saved in AutoDock assessable format with PDBQT file extension. To prepare the configuration file, a grid box was created by selecting the amino acids that constitute the active site of the protein. However, 0.375 Å spacing was applied and grid box orientation was constructed with -21.808, 60.032 and -30.852 for specifying center of X, Y, and Z coordinates respectively. We selected five additional drug compounds (Verapamil,<sup>53</sup> Loperamide,<sup>54</sup> Thioridazine,<sup>55</sup> Chlorpromazine,<sup>56</sup> and Auranofin<sup>57</sup>) as putative ligands through literature review due to their potential to inhibit ATP transport activity in multidrug-resistant bacteria. 3D conformations of these compounds with SDF file extension were retrieved from the PubChem database (<https://pubchem.ncbi.nlm.nih.gov/>).<sup>58</sup> The ligands were then converted to PDB format using Open Babel<sup>59</sup> software and subsequently uploaded to AutoDock tool, where they were converted to PDBQT format. Finally, the prepared compounds were saved as PDBQT file extension and utilized in AutoDock Vina for docking. The docking results were stored accordingly as a log file containing binding affinity score and an output file having different poses of the complex.

*Absorption, distribution, metabolism, excretion (ADME) and toxicological properties analysis.* Following docking, we assessed the Pharmacokinetic (PK) and ADME properties of our selected compounds using the open-source web-based tool called SwissADME ([www.swissadme.ch](http://www.swissadme.ch)),<sup>60</sup> which estimate the PK characteristics and drug-likeness of small compounds. Numerous molecular factors were included in this analysis, such as the number of hydrogen bond donors (nHBDs), hydrogen bond acceptors (nHBAs), molecular mass (MM) of the compounds, rule of five violations (nRB), and topological polar surface area (TPSA). Orally administered medications must adhere to drug-likeness properties to be considered pharmaceutically consistent with their bioactivity scores. In addition to ADME properties, the potential toxicity of the compounds to human organs or cells was also evaluated. Considering that perspective, the toxicity level of chosen compounds was assessed using the ProTox-3.0 online server (<https://tox.charite.de/protox3/>)<sup>61</sup> and the admetSAR web based server.<sup>62</sup>

## Results

### *Physicochemical properties and subcellular localization of hypothetical protein*

Table 1 summarizes the physicochemical properties of the HP (PBJ89160.1). According to predictions, the protein has 287 amino acids, a molecular weight of 31277.43 Daltons and with a theoretical isoelectric point (pI) of 5.11. Isoelectric point is



**Table 1.** Physicochemical properties of HP PBJ89160.1 estimated by ProtParam tool.

NO. OF AMINO ACID	MW(DA)	HALF LIFE (HR)	PI	(ASP + GLU)	(ARG + LYS)	INSTABILITY INDEX	GRAVY
287	31,277.43	30	5.11	41	33	25.98	-0.272

**Table 2.** Analysis of subcellular localization of HP PBJ89160.1.

TOOLS	SUBCELLULAR LOCATION
CELLO	Periplasmic
PSLpred	Periplasmic
BUSCA	Extracellular

pH at which the net charge on the protein is zero and at this pH the protein become less soluble, compact and stable that leads to crystallization of protein. The GRAVY index of this HP is -0.272. The negative GRAVY index suggests that the protein is soluble and hydrophilic in nature. It was predicted that the hypothetical protein's expected instability index was 25.98, indicating that the protein is stable. The protein contains Ala (A) (40, 13.9%), Arg (R) (5, 1.7%), Asn (N) (14, 4.9%), Asp (D) (20, 7.0%), Cys (C) (1, 0.3%), Gln (Q) (8, 2.8%), Glu (E) (21, 7.3%), Gly (G) (17, 5.9%), His (H) (3, 1.0%), Ile (I) (11, 3.8%), Leu (L) (26, 9.1%), Lys (K) (28, 9.8%), Met (M) (4, 1.4%), Phe (F) (14, 4.9%), Pro (P) (13, 4.5%), Ser (S) (17, 5.9%), Thr (T) (13, 4.5%), Trp (W) (4, 1.4%), Tyr (Y) (9, 3.1%), Val (V) (19, 6.6%). Alanine (40) was found to be the most prevalent amino acid residue, followed by glutamic acid (21) and aspartic acid (20) whereas Cysteine (1) was found to be the lowest. The protein is made up of 33 positively charged residues (arginine + lysine) and 41 negatively charged residues (aspartic acid + glutamic acid). 4406 atoms make up the atomic make-up, and the protein's molecular formula is  $C_{1410}H_{2198}N_{362}O_{431}S_5$ .

Bioinformatics-based predictions of protein function and genome annotation include predictions of protein subcellular localization, a crucial aspect aiding in the identification of potential therapeutic targets. The CELLO and PSLpred subcellular localization techniques identified the periplasmic region as the preferred subcellular location of our hypothetical protein, while the BUSCA server indicated localization in the extracellular region (Table 2). This finding correlates with the ProtParam analysis, where a GRAVY index value of -0.272 suggests that the protein is soluble. The subcellular localization predictions for our protein of interest show some inconsistency, with CELLO and PSLpred predicting a periplasmic location while BUSCA suggests an extracellular location. Upon examining the confidence scores, both CELLO and PSLpred provide high confidence in their periplasmic predictions. Additionally, features such as signal peptides identified using SignalP support a secretory pathway, which aligns with periplasmic localization in Gram-negative bacteria. However, BUSCA's integration of multiple predictors

highlights potential extracellular secretion, which could occur under certain conditions or in specific strains. Experimental evidence from similar proteins in related species indicates a primary periplasmic localization, supporting the predictions by CELLO and PSLpred. Given that cytoplasmic and periplasmic proteins are typically soluble, we infer that our subcellular predictions by CELLO, PSLpred are accurate. The SOSUI server determines that the protein is soluble and authenticated its solubility by the Protein Sol service to be 0.669 (Supplementary Figure 1).

### Domain and motif analysis

To uncover the conserved domain and potential functions of the protein, NCBI-CD search, ScanProsite, and InterProscan were employed. The NCBI CD search results suggest that the HP possesses a conserved membrane-associated lipoprotein domain in BLAST output. Gna1946 appeared as the most similar hit and therefore homology of PBJ89160.1. Moreover, Gna1946 shares a great deal of structural and sequence homology with the periplasmic substrate-binding domain of the ATP-binding cassette (ABC) transporter, which is in charge of absorbing methionine (MetQ) at positions 44-270. This substrate-binding domain is a member of the PBP2 superfamily of type 2 periplasmic binding fold proteins.<sup>63</sup> The PBP2 proteins act like Venus flytraps by binding their ligand in the space between their two globular subdomains, which are usually connected by a flexible hinge. These proteins are mostly involved in the absorption of small soluble substances in eubacteria and archaea. According to ScanProsite, the HP PBJ89160.1 has one motif that can be found in positions 1 through 20 of the bacterial membrane lipoprotein. These proteins are produced from a precursor signal peptide by a specific signal peptidase called signal peptidase II, which is present in lipoproteins. The peptidase identifies the cysteine residue as a component of a conserved sequence and removes upstream from the glyceride-fatty acid lipid.<sup>64-66</sup> It contains several antigenic elements that could increase the pathogenicity of the bacteria. MetQ is a part of a D-methionine permease that facilitates ATP-driven transport by binding proteins. ABC transporters' uncharacterized substrate-binding components have been found in other members of this family, namely NlpA. It has been established that the inner-membrane-anchored lipoprotein NlpA has a comparatively small function in methionine import. Pfam database identifies a domain as NIPA lipoprotein in 1-281 position, but PANTHER database predicts a domain D-methionine binding lipoprotein MetQ in 1-279 places. Methionine and ATP-driven transport systems are both used in each of these domains (Table 3).

**Table 3.** Analysis of domain, motif, and protein family of HP PBJ89160.1.

DATABASE	DESCRIPTION	INTERVAL	E-VALUE
NCBI CD search	PBP2_lipoprotein_Gna1946 Superfamily	44-270	3.39e-144
InterProscan	Lipoprotein NlPA family	1-281	N.A.
Pfam	NLPA lipoprotein; this family of bacterial lipoproteins contains several antigenic members	45-280	2.25e-105
PANTHER	D-methionine binding lipoprotein MetQ	1-279	NA
ScanProsite (motif)	Prokaryotic membrane lipoprotein	1-20	NA

**Table 4.** Analysis of BLASTp showing similarity among HP PBJ89160.1 and other proteins.

ACCESSION NO.	ORGANISM NAME	PROTEIN NAME	SCORE	PERCENTAGE IDENTITY	E-VALUE
PBJ89160.1	<i>Neisseria meningitidis</i>	Hypothetical protein CNQ34_02465c	NA	NA	NA
WP_002221629.1	<i>Neisseria meningitidis</i>	MetQ/NlpA family ABC transporter substrate-binding protein	583	100	0
WP_101087969.1	<i>Neisseria meningitidis</i>	MetQ/NlpA family ABC transporter substrate-binding protein	583	99.65	0
WP_002218060.1	<i>Neisseria meningitidis</i>	MetQ/NlpA family ABC transporter substrate-binding protein	580	99.30	0
WP_042743643.1	<i>Neisseria meningitidis</i>	MetQ/NlpA family ABC transporter substrate-binding protein	579	99.30	0
AAF42636.1	<i>Neisseria meningitidis</i>	Outer membrane lipoprotein GNA1946	583	100	0
EEZ72030.1	<i>Neisseria cinerea</i>	NLPA lipoprotein	288	95.49	0
KIC05807.1	<i>Morococcus cerebrosus</i>	Membrane protein	497	89.79	1e-175
EFC88029.1	<i>Neisseria mucosa</i> ATCC 25996	NLPA lipoprotein	497	89.79	1e-175
TCP01958.1	<i>Uruburuella suis</i>	D-methionine transport system substrate-binding protein	479	85	2e-168
UOO81404.1	<i>Uruburuella testudinis</i>	MetQ/NlpA family ABC transporter substrate-binding protein	481	86.41	2e-169

### KEGG metabolic pathway

KEGG pathway analysis reveals that the HP is likely involved in ATP hydrolysis for the active transport of a diverse range of substrates, including ions, sugars, lipids, sterols, peptides, proteins, and drugs. Specifically, the protein is implicated in D-amino acid metabolism, particularly in cysteine and methionine metabolism (Supplementary Figure 2).

### Phylogenetic and protein family analysis

BLASTp was used to search the non-redundant database; the results showed sequence similarities (up to 96%) with other

MetQ/NlpA family ABC transporter substrate-binding regions (Table 4). To see the conserved and different residues among the homologs, multiple sequence alignments were performed using the BLASTp (Figure 2) which revealed a detailed

Comparative analysis of the hypothetical protein from *Neisseria meningitidis* against various homologous and related proteins from different bacterial species. PBJ89160.1 is highly homologous to several other MetQ/NlpA family ABC transporter substrate-binding proteins within *Neisseria meningitidis*, indicating that it likely performs a similar role in substrate binding and transport. The high sequence identity to other ABC transporter proteins supports the hypothesis that

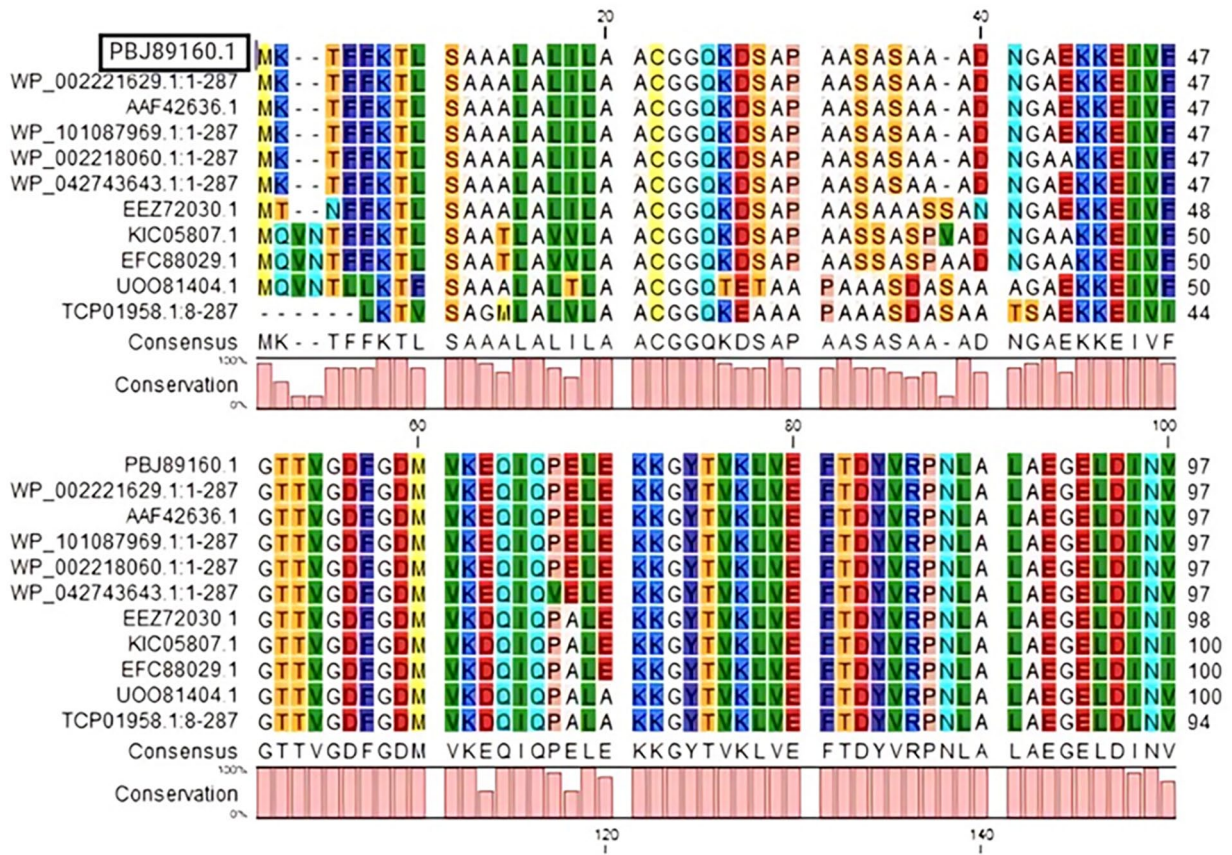


**Figure 2.** Multiple sequences alignment analysis. Source: For the sequences: Rows 2, 3, 4, 5, 6, *Neisseria meningitidis*; Row 7, *Neisseria cinerea*; Row 8, *Morococcus cerebrosus*; Row 9, *Neisseria mucosa*; Row 10, *Uruburuella testudinis*; Rows 11, *Uruburuella suis*. Version 8 of CLC Sequence Viewer was used. Multiple sequences alignment of various methionine uptake system proteins, with the target protein in the top row.

PBJ89160.1 is involved in methionine transport, contributing to the bacterium’s virulence by aiding in nutrient uptake. Proteins from other species show varying degrees of similarity, with the closest homologs being from other *Neisseria* species and more distant homologs from unrelated bacteria. This further suggests that while PBJ89160.1 is well- conserved within the *Neisseria* genus, it has more divergent homologs in other genera. The same data was used to construct a phylogenetic tree (Figure 3). Phylogenetic analysis revealed that the HP appears to share a common ancestor with WP002221629.1 and AAF42636.1 proteins of *N. meningitidis*.

*Protein interaction map*

A STRING 12.0 search was conducted to identify the potential functional interaction network of the HP PBJ89160.1 (Figure 4). The analysis revealed several significant interactions with other proteins, including NMB1947 (score: 0.999), NMB1948 (score: 0.999), frpC (score: 0.649), NMB0938 (score: 0.527), NMB1483 (score: 0.465), PilB (score: 0.436), metG (score: 0.435), metF (score: 0.562), metK (score: 0.765), and metH (score: 0.589). Among these, NMB1946 predominantly interacts with NMB1947 and NMB1948, which are involved in methionine import. Other identified partners include an iron-regulated protein, two hypothetical proteins, L-methionine-(S)-S-oxide

reductase, methionyl-tRNA synthetase, 5,10-methylenetetrahydrofolate reductase, S-adenosylmethionine synthetase, and 5-methyltetrahydropteroyltriglutamate-homocysteine methyltransferase (Figure 4). The analysis encompassed parameters such as the number of nodes (12), edges (32), average node degree (3.56), average local clustering coefficient (0.536), and protein-protein interaction enrichment p-value (0.034).

*Secondary structure prediction*

The SOPMA server was used to determine the percentages of the HP secondary structures including alpha helix (42.51%), random coil (33.80%), extended strand (16.03%), and beta turn (7.67%). A similar outcome was obtained in the PSIPRED study (Figure 5).

*Determination of the three-dimensional structure*

3D structure of the hypothetical protein was ascertained using the template outer membrane lipoprotein GNA1946 (PDB\_ID: 3GXA), which showed 99% identity with our HP in the HHpred server. To visualize the structure, BIOVIA Discovery Studio Visualizer was utilized (Figure 6A). Utilizing UCSF Chimera software, the superimposition of the HP PBJ89160.1 and template protein 3GXA was



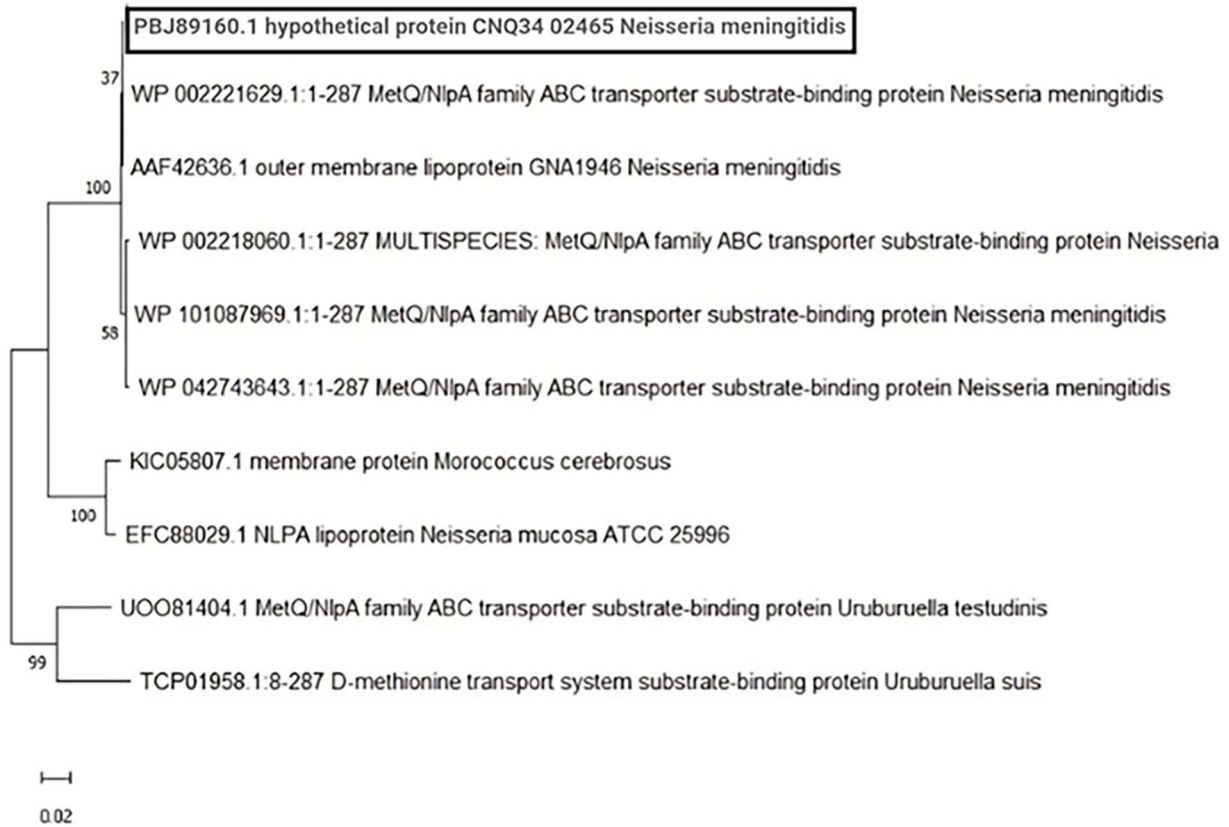


**Figure 3.** Phylogenetic tree with genuine distance to HP PBJ89160.1.

MEGA 11 version was used to create the tree. The line segment with the number (0.02) on it represents the amount of genetic alteration, and the scale bar in this case estimates the degree of sequence divergence.

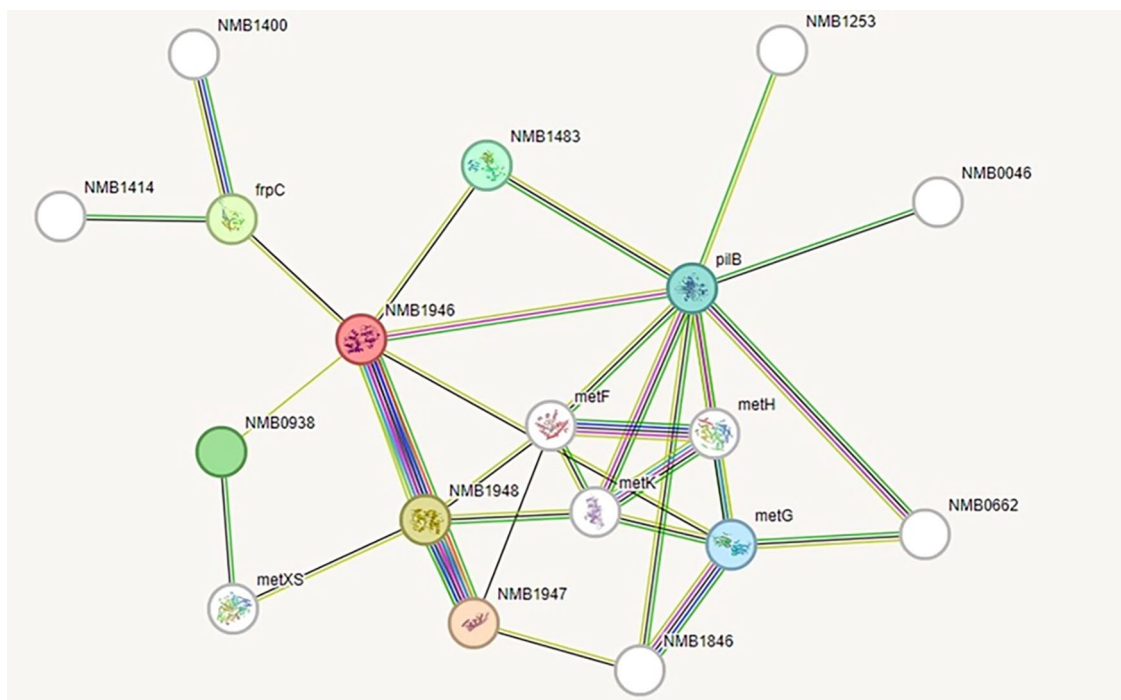


**Figure 4.** Protein-protein interaction network analysis by STRING.

Here, NMB1946 is the HP PBJ89160.1 under study in this STRING network analysis.



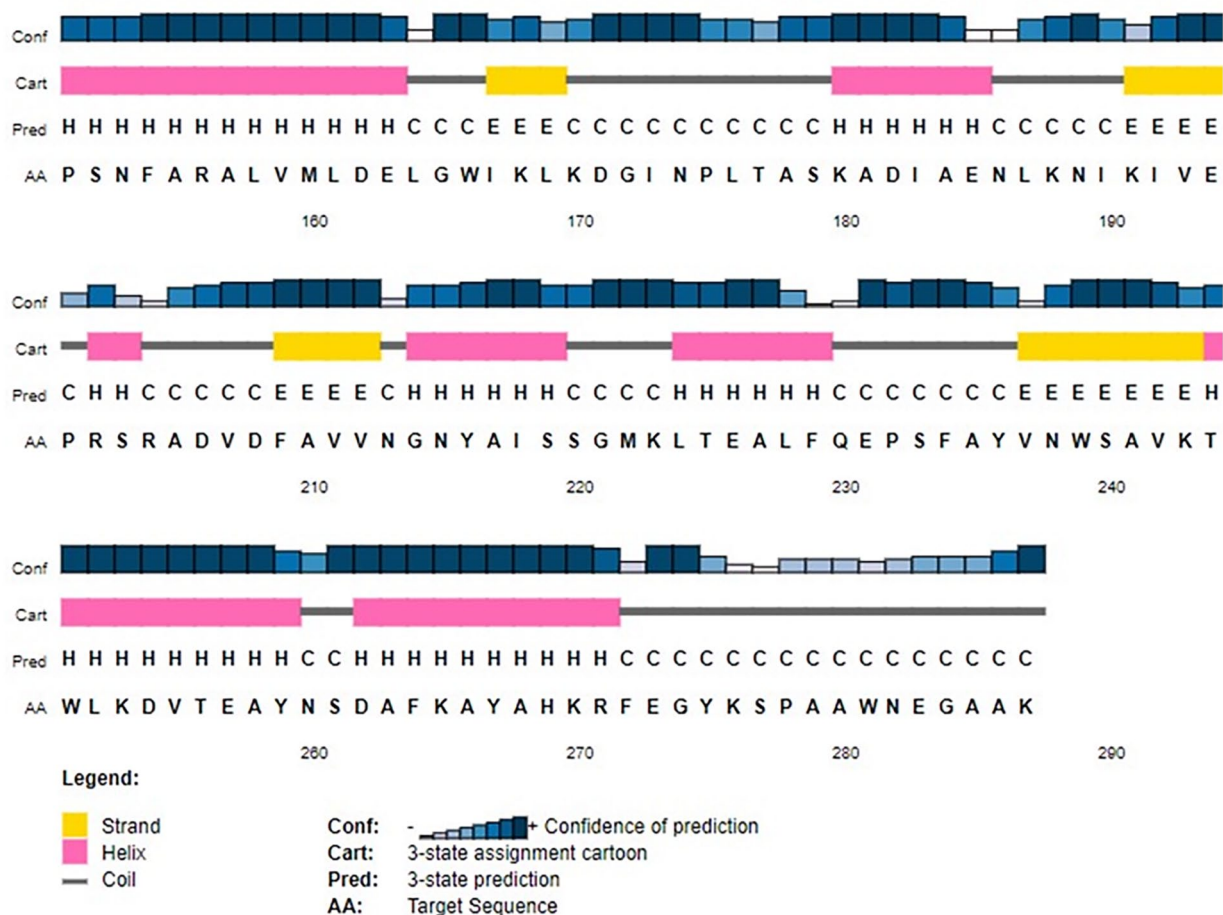


**Figure 5.** Secondary structure of HP PBJ89160.1.

PSI-PRED server predicted the target protein's secondary structure. Four distinct components make up this graphic illustration. Bars in the first part are varied heights. The confidence score is proportional to the length of the bar height. In the second section, the alpha helix is represented by the pink color, the beta sheets or strands are represented by the yellow color, and the coils are represented by the gray color. A coil links a specific beta sheet to a specific alpha helix. The secondary structure of a protein is depicted alphabetically in the third section; here, the letters E, H, and C stand in for beta sheets, alpha helices, and coils, respectively. The order of amino acids is listed alphabetically in the final section.

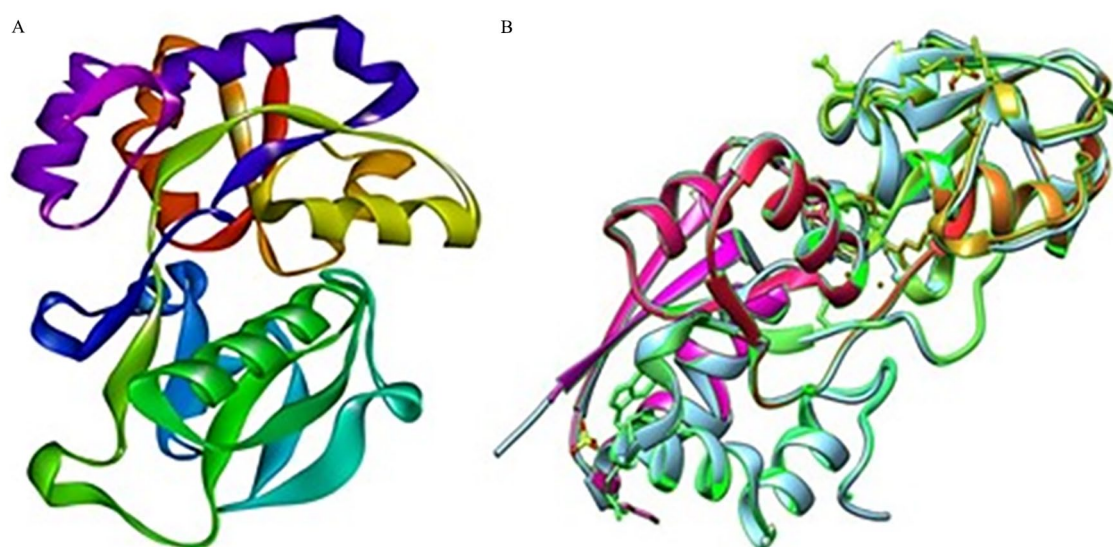


**Figure 6.** Three-dimensional structure prediction of HP PBJ89160.1 and superimposition with template protein. Here, (A) HHpred server's prediction of the hypothetical protein's three-dimensional structure (shown by BIOVIA Discovery Studio Visualizer version 20.1.0.19295). (B) Superimposition of the HP (PBJ89160.1) and template protein by UCSF chimera software.

**Table 5.** Ramachandran plot statistics of HP PBJ89160.1.

STATISTICS	NO. OF AA RESIDUES (%)
Residues in the most favored regions [A, B, L]	203 (94)
Residues in additional allowed regions [a, b, l, p]	13 (6)
Residues in generously allowed regions [~a, ~b, ~l, ~p]	0 (0)
Residues in disallowed regions	0 (0)
No. of non-glycine and non-proline residues	Total 216 (100)
No. of end residues (excl. Gly and Pro)	2
No. of glycine residues (shown in triangles)	13
No. of proline residues	12
Total no. of residues	243

conducted, as illustrated in (Figure 6B). LIGPLOT analysis from PDBsum server showed the detailed protein ligand interactions (Supplementary Figure 3).

#### *Energy minimization of predicted hypothetical protein 3D structure*

The three-dimensional structure of the HP was subjected to energy minimization using the YASARA force field minimizer. As a result of this process, the energy level was reduced from  $-108,282$  kJ/mol to  $-141,099.1$  kJ/mol. Despite this significant energy reduction, the final value changed from  $-0.8$  to  $0.4$ , indicating a stable structure.

#### *Evaluation of the model quality*

After energy minimization, the quality of the stable 3D structure of HP was assessed using PROCHECK analysis. Specifically, the Ramachandran plot indicated that 94% of the amino acid residues are located in the most favored regions, signifying a high level of structural acceptability (Table 5, Figure 7A). Upon analysis of the Verify 3D plot, we determined that 88.70% of residues exhibited an average  $3D-1D \geq 0.1$ . It is inferred that at least 80% of the amino acids have scored  $\geq 0.1$  in the 3D-1D profile for being the structure of the protein to be stable. Therefore, the HP in the study is stable. The ERRAT software assigned an overall quality factor of 92.3404 to the predicted protein model, and the QMEAN4 score further gauges model reliability by comparing its structure to previously established experimental structures of similar sizes. The QMEAN4 global score for our hypothetical protein is  $-0.75$ , indicating a favorable model quality (Figure 7B). The Z score of a model serves as an indicator of its overall quality and is used to assess whether the input structure falls within the typical range observed for

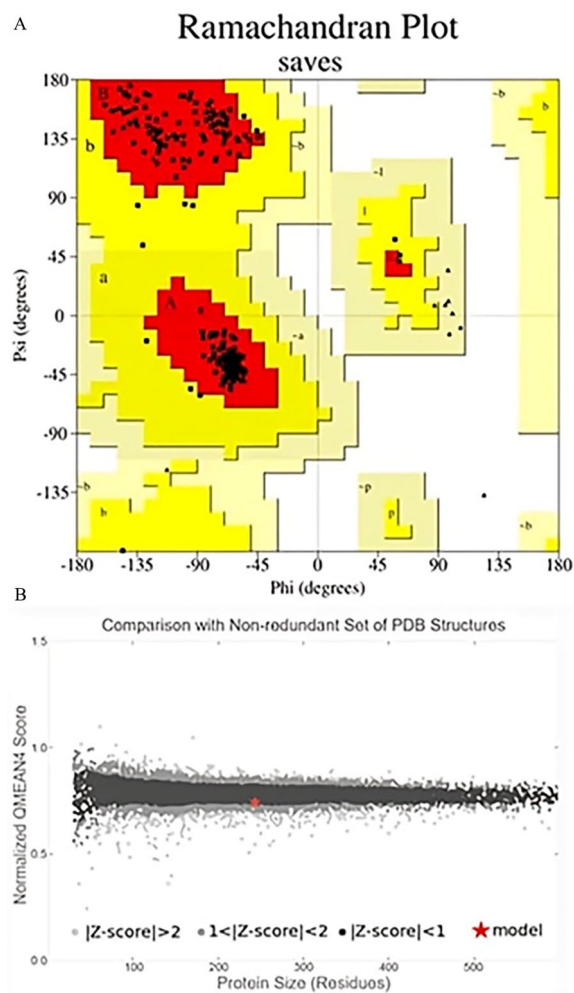


**Figure 7.** Evaluation of the model's quality of HP PBJ89160.1 three-dimensional structure. Here, (A) The PROCHECK program-validated Ramachandran plot of the model structure and (B) the graphic representation of the model's QMEAN result show that the model structure and experimental structures of comparable size ( $-0.75$ ) are in good agreement.

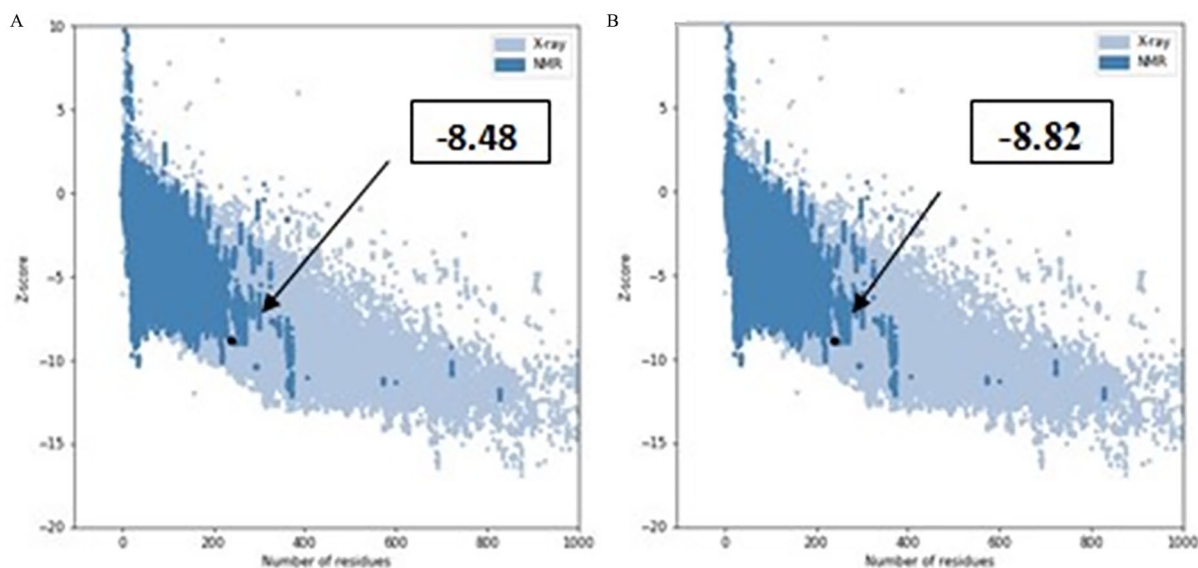


**Figure 8.** Z scores of the Model HP PBJ89160.1. Here, (A) is structure of HP PBJ89160.1 and (B) template protein. The locations of the two structures were typical for natural proteins of similar size that have been determined experimentally (by NMR and X-ray).

native proteins of similar size. In this study, a Z score of  $-8.48$  for the model HP (Figure 8A) and  $-8.82$  for the template (Figure 8B), suggesting significant homology between the template and the modeled structure. The root-mean-square deviation (RMSD) between 239 pruned atom pairs was measured at 0.449 angstroms, consistently observed across all 239 pairs. The protein is further validated with VoronoiQA server in which the validation score is 0.507 that indicates a good protein quality as per global VoronoiQA score (Supplementary Figure 4).

#### Active site analysis

In the development of a drug or inhibitor to target a protein, it is crucial to identify the protein's active site. The CASTp server was employed to determine the active site in the 3D structure (Figure 9). One of the largest pockets revealed the most active site, with a total volume of 58.983 amino acids and a solvent-accessible (SA) surface area of 92.084, respectively. The pocket revealed key active residues are THR<sup>79</sup>, ASP<sup>80</sup>, ASP<sup>80</sup>, TYR<sup>81</sup>, TYR<sup>81</sup>, TYR<sup>81</sup>, VAL<sup>82</sup>, TYR<sup>103</sup>, TYR<sup>103</sup>, PRO<sup>148</sup>, ASN<sup>149</sup>, ASP<sup>150</sup>, ASP<sup>150</sup>, ASP<sup>150</sup>, ASN<sup>153</sup>, ASN<sup>153</sup>, GLU<sup>196</sup>, GLU<sup>196</sup>, GLU<sup>196</sup>, GLU<sup>196</sup>, GLU<sup>196</sup>, ALA<sup>197</sup>, ALA<sup>197</sup>, ALA<sup>198</sup>, ALA<sup>198</sup>, ASN<sup>213</sup>, and TYR<sup>216</sup>.

#### Molecular docking

Molecular docking results explore the binding affinity among five tentative drug compounds aforementioned earlier and to the selective hypothetical protein. Interestingly, the natural compound, Methionine was exhibited the lowest binding affinity ( $-4.9$  kcal/mol) where the highest binding affinity was calculated for Loperamide ( $-7.6$  kcal/mol). Thus, molecular docking analysis successfully anticipated a receptor-ligand

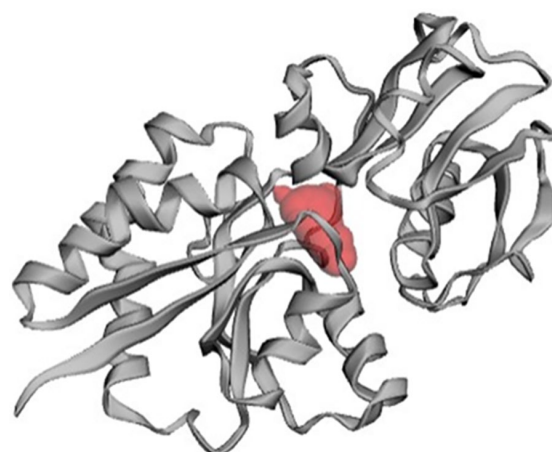


**Figure 9.** Prediction of active site of HP PBJ89160.1. The HP's PBJ89160.1 active site is determined by CASTp server. The largest active site was found in the areas with 92.084 and volume of 58.983 amino acids.

complex having the strongest binding affinity. However, rests of the calculated energies of other drug compounds with the same hypothetical protein through docking analysis are summarized in Table 6. Visualization of the top scored complex was done by accessing docked structures having nine different poses. More the hydrogen bonds are present in the complex meaning the docking complex is more preferable as well as fitted for drug discovery.<sup>67</sup> The highest number of interacting residues was observed in the interaction of Loperamide and HP where a single hydrogen bond interacted to His<sup>111</sup> with an oxygen radical (from 2.2 Å) of Loperamide. Moreover, Val<sup>82</sup> was interacted via pi-alkyl bond combining with cyclohexane ring (from 4.7 Å) and benzene ring (from 5.3 Å). Similarly, Pro<sup>151</sup> were interacted via pi-alkyl bond with nitrogen atom found in the middle of the Loperamide structure distancing from 4.4 Å. Tyr<sup>103</sup> and Glu<sup>110</sup> were contracted



**Table 6.** Binding affinity among five therapeutic compounds and HP PBJ89160.1.

TARGET PROTEIN	LIGAND(S)	PUBCHEM ID	BINDING AFFINITY (KCAL/MOL)
Hypothetical protein	Methionine (MetQ)		-4.9
	Verapamil	2520	-6.8
	Loperamide	3955	-7.6
	Thioridazine	5452	-6.4
	Chlorpromazine	2726	-5.4
	Auranofine	24199313	-5.1

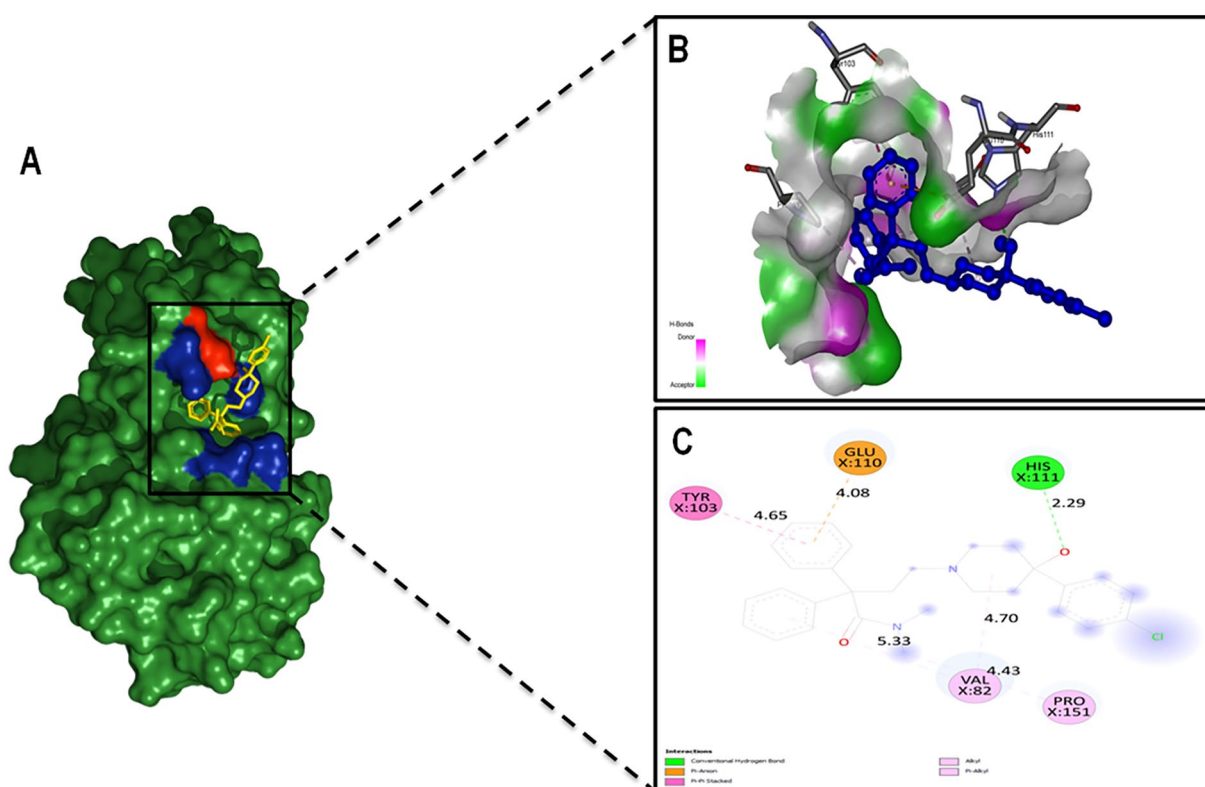


**Figure 10.** Molecular docking analysis showing the best pose of HP with Loperamide. (A) Protein-ligand interaction with surface representation. Red and blue color surrounding to ligand (yellow) depicted polar and non-polar residues, respectively. (B) An enhanced 3D illustration showed ligand-binding pocket. (C) 2D image showing interactions between receptor and substrate via one conventional hydrogen bond distancing 2.29 Å and two Pi-Alkyl bonds. A single pi-anion and a pi-pi stacked found interacting with a benzene ring of Loperamide.

with pi-pi- stacked and pi-anion bond respectively. In this case, another benzyl group found in ligand compound is the interacting structure that is connected with two amino acid residues distancing from 4.6 Å to 4 Å respectively (Figure 10).

#### *ADMET analysis and toxicity prediction of the selected drug compounds*

The canonical SMILES of the five compounds were analyzed using the SwissADME web tool. Table 7 presents the physicochemical properties of these compounds, indicating their potential as pharmaceuticals. Table 8 details the

predicted toxicological properties, derived using the admet-SAR server. The findings reveal that CID 24199313 is toxic according to the Ames test. However, all compounds were identified as weak inhibitors of the human ether-a-go-go-related gene (hERG) and exhibited low rat acute toxicity, with a median lethal dose (LD<sub>50</sub>) of 2.35 mol/kg. Based on the ADMET prediction profile, compounds were categorized into four groups based on acute oral toxicity: Group I (LD<sub>50</sub> ≤ 50 mg/kg), Group II (50 < LD<sub>50</sub> ≤ 500 mg/kg), Group III (500 < LD<sub>50</sub> ≤ 5000 mg/kg), and Group IV (LD<sub>50</sub> > 5000 mg/kg). According to the predicted acute oral toxicity values, compounds CID 2520, CID 3955, and CID

**Table 7.** Pharmacokinetic properties of selected five therapeutic compounds.

PUBCHEM ID		CID 2520	CID 3955	CID 5452	CID 2726	CID 24199313
Physiochemical properties	Molecular weight (g/mo)	454.60	477.04	370.57	318.86	678.48
	Heavy atoms	33	34	25	21	32
	Arom. heavy atoms	12	18	12	12	0
	Rotatable bond	13	8	4	4	12
	H-bond acceptor	6	3	1	1	9
	H-bond donor	0	1	0	0	0
Lipophilicity	Log Po/w	4.50	4.06	4.03	3.47	0.00
Water solubility	Log S (ESOL)	-4.46	-5.82	-5.95	-5.25	-4.55
Pharmacokinetics	GI absorption	High	High	High	High	High
Drug likeliness	Lipinski	Yes	Yes	Yes	Yes	Yes
Medical chemistry	Synthetic accessibility	Easy	Easy	Easy	Easy	Easy

**Table 8.** Toxicological properties of predicted five therapeutic compounds.

COMPOUND (PUBCHEM ID)	HERG INHIBITION	RAT (LD50)	AMES TEST	CARCINOGENS	ACUTE ORAL TOXICITY	CARCINOGENICITY (THREE CLASS)
2520	Weak	3.4137	No	No	II	Not required
3955	Weak	3.6560	No	No	II	Not required
5452	Weak	2.5395	No	No	III	Not required
2726	Weak	3.3196	No	No	II	Not required
24199313	Weak	2.7163	Toxic	No	III	Not required

**Table 9.** Toxicity profiling of top five predicted therapeutic compounds through ProTox-3.0 server.

COMPOUND (PUBCHEM ID)	CYTOTOXICITY	IMMUNOTOXICITY	MUTAGENECITY	CARCINOGENECITY
2520	Inactive	Active	Inactive	Inactive
3955	Inactive	Inactive	Inactive	Inactive
5452	Inactive	Active	Inactive	Inactive
2726	Inactive	Active	Inactive	Inactive
24199313	Inactive	Inactive	Inactive	Inactive

2726 fall within Class II, while compounds CID 5452 and CID 24199313 fall within Class III. These classifications indicate that the compounds are generally suitable for drug development, with LD50 values less than 5000 mg/kg.

To further validate the toxicity profiles, the ProTox 3 web server was employed (Table 9). The analysis identified three compounds (CID 2520, CID 5452, and CID 2726) as immunotoxic. After evaluating all the properties, CID 3955 (Loperamide) emerged as the best fit against our hypothetical protein HP (PBJ89160.1). The graphical interaction between HP and Loperamide is depicted in Figure 10.

## Discussion

*Neisseria meningitidis* is the causative agent of major meningococcal disease outbreaks and high morbidity rates. Additionally, the emergence of multiple antibiotic-resistant strains due to improper antibiotic use has made treating meningococcal disease more challenging. Therefore, identifying alternative therapeutic targets is essential to combat this bacterial infection. In many studies it was reported that HPs of an organism could serve as valuable sources for alternative therapeutic targets.<sup>68-71</sup> Therefore, characterizing HP (PBJ89160.1) from *N. meningitidis* can enhance our understanding of bacterial metabolic

regulation, aid in formulating disease control strategies, and contribute to the development of effective therapeutics. The characterization of this hypothetical protein involved the sequential application of various bioinformatics tools. Functional analysis, conducted using NCBI CD Search, ScanProsite, InterProscan, Pfam, and PANTHER, suggests that the protein may exhibit D-methionine absorption activity and possess several antigenic characteristics. The 3D structure of the protein was modeled using the HHpred server, employing a template (3GXA; GNA1946 outer membrane lipoprotein) with over 99% similarity. GNA1946 is a type of lipoprotein and one of the first ABC transporter family members. It has a strong affinity and specificity towards L-methionine, and it is believed to bind to it instead of D-methionine. Pathogens, through nutritional assimilation, such as scavenging amino acids for protein synthesis, adapt and survive within their niches. They employ “nutritional virulence” mechanisms to augment the host’s acquisition of limited nutrients by specifically targeting key host biosynthetic pathways or nutrient-rich sources.<sup>72</sup> The amino acid uptake function is a major research target. The protein is a substrate binding protein (SBP) that interacts with microvascular endothelial cells in the human brain, possibly functioning as an adhesion that is periplasmically localized and absorbs methionine.<sup>73</sup> This nutritional virulence is caused by ABC Transporter family proteins and our HP belongs to this family. Meanwhile, ABC transporters are used as (1) Target for antimicrobials-by designing antibiotics that mimic transporter substrates specifically that have broad specificity for substrate binding, (2) target for drug development by designing inhibitors that target components of the transporters, essential for survival and act as nutritional virulence factors, and (3) target for vaccine development-by designing vaccine against transporter proteins.<sup>74</sup>

The main focus of the study is to advance the understanding of the HP from *Neisseria meningitidis*, particularly in terms of its structural and functional characteristics, and to explore its potential as a target for therapeutic intervention in treating bacterial meningitis. Therefore, it is a prerequisite to know about the function of domain and motif of the protein. The NCBI CD search analysis revealed that HP (PBJ89160.1) is composed of multiple enzyme families that serve as substrate-binding domains and are members of the type 2 periplasmic binding fold protein superfamily (PBP2). These enzyme families share structural similarities. The bulk of PBP2 proteins work in eubacteria and archaea to take up tiny soluble substrates. The HP has one motif, which is bacterial membrane lipoprotein, according to ScanProsite. Previous studies demonstrated that a precursor signal peptide is used in the synthesis of these proteins. Signal peptidase II, a key component of lipoproteins, is responsible for cleaving the signal peptide.<sup>65</sup>

The CLC sequence viewer was utilized for generating multiple sequence alignment, and MEGA software facilitated phylogenetic tree analysis. The HP is homologous to two

proteins, one of which functions as ABC transporter SBP (WP002221629.1) and another is outer membrane lipoprotein GNA1946 (AAF42636.1) in *N. meningitidis*. Protein-protein interaction is commonly used to detect the interactive functional proteins in a signaling pathway which reveals the cellular mechanism of an organism.<sup>75</sup> In STRING analysis it was observed that HP PBJ89160.1 protein interacts with ten other proteins. Among them higher interaction was observed with two proteins (NMB1947, NMB1948) that has methionine importer activity. According to STRING database, NMB1947 is involved in D-methionine transmembrane transport and NMB1948 is an ABC transporter, ATP-binding protein; Part of the ABC transporter complex. MetNIQ involved in methionine import, responsible for energy coupling to the transport system and belongs to the ABC transporter superfamily. The HP PBJ89160.1 protein also showed comparable function with NMB1947 and NMB1948.

In the quality analysis, the ProCheck server revealed reliable scores for the Ramachandran plot, Verify 3D, ERRAT, and Qmean value, indicating that the structure is likely significant.<sup>76</sup> According to the global Voronoi score, protein’s having more than 0.4 score validated as good quality protein and our protein’s Voronoi score is 0.507 predicted as good protein quality. The modeled protein’s 3D structure was refined using Discovery Studio, which removed all water molecules and docked the protein with its natural ligand, methionine. The binding affinity between the hypothetical protein and methionine was found to be  $-4.9$  kcal/mol.

There are some reports where ADMET and Pharmacophore characterization approaches were used to predict the best drug candidate.<sup>77</sup> Aiming to identify potential therapeutic compounds that could inhibit the molecular function of the HP (PBJ89160.1), we selected five candidate drugs for further analysis. These compounds were docked with the modeled HP (PBJ89160.1) to assess their binding affinities. Subsequent ADME and toxicological properties analyses led to the elimination of four drugs due to their toxic properties. Only one drug, Loperamide, met all the criteria. Loperamide demonstrated a binding affinity of  $-7.6$  kcal/mol with the HP (PBJ89160.1), making it the most promising drug candidate against the protein. P-glycoprotein (P-gp) is an ATP-dependent efflux transporter, and loperamide is found to be inhibiting its function. P-gp plays a crucial part in the absorption and disposal of drugs by expelling different substances, including drugs, from cells.<sup>78</sup> The quick uptake and efflux of medications across the cell membrane is facilitated by the P-gp, one of the proteins that make up the ATP-binding cassette transporter family.<sup>79</sup> Therefore, our candidate drug Loperamide could play potential vital role in the treatment of meningococcal disease.

Finally, human homologous research using BLAST revealed that the chosen protein does not homologous to humans. As a result, there are no longer any odds of an adverse consequence, proving that this protein may be a good therapeutic target. It’s



expected that additional functional and structural research on the ABC transporters of Gram-negative bacteria will shed light on their as-yet-unidentified transport mechanism. Despite this, our findings are helpful in creating broad-spectrum vaccinations to protect against the bacterium *N. meningitidis*.<sup>80</sup>

## Conclusion

In conclusion, this study has successfully characterized a new HP, which is believed to play a crucial role in nutritional virulence and the ABC transport mechanism as a methionine transporter. However, further experimental validation and functional characterization are necessary to confirm its predicted structural and functional attributes. There are several in vitro studies like (Gene expression analysis, protein-protein interaction, enzyme assay, and cell based assay) and in vivo studies like (animal model, disease model, histopathological studies) can be conducted to verify the protein's function and potential as drug target. To build on these findings, we recommend conducting additional immune-informatics and structural biology methodologies, alongside in vitro and in vivo studies, to thoroughly understand and validate the drug targets against meningitis. Nonetheless, this discovery lays a strong foundation for further research aimed at understanding the genetic and proteomic profile of *N. meningitidis* and identifying potential drug targets. Such comprehensive studies are essential due to the inherent limitations of in silico models, which struggle to fully capture the complexity of biological systems, individual genetic variations, and environmental influences on drug response.


## Acknowledgements

The authors acknowledge the Department of Biotechnology and Genetic Engineering, Noakhali Science and Technology University for providing support to conduct the research work.

## Author Contributions

Conceptualization: IJA, SDG & DNB; Data curation: IJA & DNB; Formal analysis: IJA, SDG, MMH & DNB; Supervision: DNB; Software: IJA, MNI & NNA; Resources: DNB; Writing original draft: IJA, SDG, NNA & DNB; Writing, review and editing: SDG, MMH, MMI, SCD, MNI & DNB.

## ORCID iDs

Md. Murad Hossain  <https://orcid.org/0009-0002-0852-9737>

Dhirendra Nath Barman  <https://orcid.org/0000-0002-7086-976X>

## Supplemental Material

Supplemental material for this article is available online.

## REFERENCES

1. Yazdankhah SP, Caugant DA. *Neisseria meningitidis*: an overview of the carriage state. *J Med Microbiol*. 2004;53:821-832.

2. Manchanda V, Gupta S, Bhalla P. Meningococcal disease: history, epidemiology, pathogenesis, clinical manifestations, diagnosis, antimicrobial susceptibility and prevention. *Indian J Med Microbiol*. 2006;24:7-19.
3. Batista RS, Gomes AP, Luiz J, Gazinco JLD, Paulo S, Miguel PSB, Santana LA, Olivera L, Geller M. Meningococcal disease, a clinical and epidemiological review. *Asian Pac J Trop Med*. 2017;10:1019-1029.
4. Lacey RW, Reeves DS, Emilio P, Aldamiz-echeverria L, Eduardo GP. Meningococci with increased resistance to penicillin. *Lancet*. 1989;23:8220.
5. Mastrantonio TSMECMO and P. Meningococcal disease in Italy. *J Infect*. 1989;19:69-74.
6. Tzanakakp G, Blackwell CC, Kremastinou J. Antibiotic sensitivities of *Neisseria meningitidis* isolates from patients and carriers in Greece. *Epidemiol Infect*. 1992;108:449-455.
7. Greenhouse P, Howell PR. Penicillin-insensitive *Meningococci* in the UK. *Lancet*. 1988;331:657-658.
8. Woods CR, Smith AL, Wasilaukas BL, Campos J, Givner LB. Invasive disease caused by *Neisseria meningitidis* relatively resistant to Penicillin in North Carolina. *J Infect Dis*. 1994;170:453-456.
9. Oppenheim BA. Antibiotic resistance in *Neisseria meningitidis*. *Clin Infect Dis*. 1991;24:98-101.
10. Khoosal M. Susceptibility of *Neisseria meningitidis* in Israel to penicillin and other drugs of interest. *J Antimicrob Chemother*. 1993;32:166-168.
11. Greenwood BM, Blakebrou GH, Dagger IS, Bradley AK, Wali S, Whittle HC. Meningococcal disease and season in Sub-Saharan Africa. *Lancet*. 1984;323:1339-1342.
12. Stephens DS, Sherman AC, Stephens DS, Sherman AC, Serogroup A. Serogroup A meningococcal conjugate vaccines: building sustainable and equitable vaccine strategies. *Expert Rev Vaccines*. 2020;19:455-463.
13. Tzeng Y ling, Stephens DS. Epidemiology and pathogenesis of *Neisseria meningitidis*. *Int J Epidemiol*. 2000;29:687-700.
14. Jackson LA, Schuchat A, Reeves MW, Wenger JD. Serogroup C meningococcal outbreaks in the United States. An emerging threat. *JAMA*. 1995;273:383-389.
15. Jafri RZ, Ali A, Messonnier NE, et al. Global epidemiology of invasive meningococcal disease. *Popul Health Metr*. 2013;11:1-9.
16. Moore PS, Schwartz B, Reeves MW, Gellin BG, Broome CV. Intercontinental spread of an epidemic group a *Neisseria meningitidis* strain. *Lancet*. 1989;334:260-263.
17. WHO. *Defeating Meningitis by 2030 a Global Road Map*. 2021.
18. Mills CL, Beuning PJ, Ondrechen MJ. Biochemical functional predictions for protein structures of unknown or uncertain function. *CSBJ*. 2015;13:182-191.
19. Siddiqui Q, Ali MSM, Leow ATC, Oslan SN, Mohd Shariff F. In silico identification and characterization of potential druggable targets among hypothetical proteins of *Leptospira interrogans* serovar Copenhageni: a comprehensive bioinformatics approach. *J Biomol Struct Dyn*. 2023;41:10347-10367.
20. Naveed M, Tehreem S, Usman M, Chaudhry Z, Abbas G. Structural and functional annotation of hypothetical proteins of human adenovirus: prioritizing the novel drug targets. *BMC Res Notes*. 2017;10:706.
21. Passalacqua KD, Charbonneau M, Riordan MXDO. Bacterial metabolism shapes the host – pathogen interface. In: Kudva IT, Cornick NA, Plummer PJ, et al, eds. *Virulence Mechanisms of Bacterial Pathogens*. Wiley; 2016:15-41.
22. Gasteiger E, Hoogland C, Gattiker A, et al. Protein identification and analysis tools on the ExPASy server. In: Walker JM, ed. *The Proteomics Protocols Handbook*. Humana Press; 2005;112:531-552.
23. Sheng YC, Jen LC. Predicting subcellular localization of proteins for Gram-negative bacteria by support vector machines based on n-peptide compositions. *Protein Sci*. 2004;13:1402-1406.
24. Bhasin M, Garg A, Raghava GPS. PSLpred: prediction of subcellular localization of bacterial proteins. *Nucleic Acids Res*. 2005;21:2522-2524.
25. Savojardo C, Martelli PL, Fariselli P, Profti G, Casadio R. BUSCA: an integrative web server to predict subcellular localization of proteins. *Nucleic Acids Res*. 2018;46:459-466.
26. Hirokawa T, Boon-Chieng S, Mitaku S. SOSUI: classification and secondary structure prediction system for membrane proteins. *Bioinformatics*. 1998;14:378-379.
27. Hebditch M, Carballo-Amador MA, Charonis S, Curtis R, Warwicker J. Protein-Sol: a web tool for predicting protein solubility from sequence. *Bioinformatics*. 2017;33:3098-3100.
28. Lu S, Wang J, Chitsaz F, et al. CDD/SPARCLE: the conserved domain database in 2020. *Nucleic Acids Res*. 2020;48:D265-D268.
29. Quevillon E, Silventoinen V, Pillai S, et al. InterProScan: protein domains identifier. *Nucleic Acids Res*. 2005;33:116-120.
30. Cuche A, Sigrist CJA, Castro E De, et al. New and continuing developments at PROSITE. *Nucleic Acids Res*. 2013;41:344-347.
31. Kanehisa M, Furumichi M, Tanabe M, Sato Y, Morishima K. KEGG: new perspectives on genomes, pathways, diseases and drugs. *Nucleic Acids Res*. 2017;45:D353-D361.
32. Szklarczyk D, Kirsch R, Koutrouli M, et al. The STRING database in 2023: protein – protein association networks and functional enrichment analyses for any sequenced genome of interest. 2023;51:638-646.

33. Johnson M, Zaretskaya I, Raytselis Y, Merezhuk Y, McGinnis S, Madden TL. NCBI BLAST: a better web interface. *Nucleic Acids Res.* 2008;36:5-9.
34. Tamura K, Stecher G, Kumar S. MEGA11: molecular evolutionary genetics analysis version 11. *Mol Biol Evol.* 2021;38:3022-3027.
35. Geourjon C, Deleage G. SOPMA: significant improvements in protein secondary structure prediction by consensus prediction from multiple alignments. *Bioinformatics.* 1995;11:681-684.
36. McGuffin LJ, Bryson K, Jones DT. The PSIPRED protein structure prediction server. *Bioinformatics.* 2000;16:404-405.
37. Robert X, Gouet P. Deciphering key features in protein structures with the new ENDscript server. *Nucleic Acids Res.* 2014;42:320-324.
38. Webb B, Sali A. Protein structure modeling with MODELLER. *Methods Mol Biol.* 2014;1137:1-15.
39. Biovia DS. *Discovery Studio Visualizer.* Vol. 936. Dassault Systèmes; 2017:240-249.
40. Thornton JM. PDBsum: structural summaries of PDB entries. *Protein Sci.* 2018;27:129-134.
41. Söding J, Biegert A, Lupas AN. The HHpred interactive server for protein homology detection and structure prediction. *Nucleic Acids Res.* 2005;33:244-248.
42. Tian W, Chen C, Lei X, Zhao J, Liang J. CASTp 3.0: computed atlas of surface topography of proteins. *Nucleic Acids Res.* 2018;46:W363-W367.
43. Laskowski RA, Rullmann JA, MacArthur MW, Kaptein R, Thornton JM. AQUA and PROCHECK-NMR: programs for checking the quality of protein structures solved by NMR. *J Biomol NMR.* 1996;8:477-486.
44. Eisenberg D, Lüthy R, Bowie JU. VERIFY3D: assessment of protein models with three-dimensional profiles. In: Lüthy R, Bowie J, Eisenberg D, eds. *Methods in Enzymology.* Academic Press; 1997;277:396-404.
45. Benkert P, Biasini M, Schwede T. Toward the estimation of the absolute quality of individual protein structure models. *Bioinformatics.* 2011;27:343-350.
46. Colovos C, Yeates TO. Verification of protein structures: patterns of nonbonded atomic interactions. *Protein Sci.* 1993;2:1511-1519.
47. Pettersen EF, Goddard TD, Huang CC, et al. UCSF Chimera – a visualization system for exploratory research and analysis. *J Comput Chem.* 2004;25:1605-1612.
48. Wiederstein M, Sippl MJ. ProSA-web: interactive web service for the recognition of errors in three-dimensional structures of proteins. *Nucleic Acids Res.* 2007;35:407-410.
49. Olechnovi K. VoroMQA web server for assessing three-dimensional. *Nucleic Acids Res.* 2019;47:437-442.
50. Trott O, Olson AJ. AutoDock Vina: improving the speed and accuracy of docking with a new scoring function, efficient optimization, and multithreading. *J Comput Chem.* 2010;31:455-461.
51. Yang X, Wu Z, Wang X, Yang C, Xu H, Shen Y. Crystal structure of lipoprotein GNA1946 from *Neisseria meningitidis*. *J Struct Biol.* 2009;168:437-443.
52. Schrodinger LL. *The PyMOL Molecular Graphics System.* Version 1. 2015:8.
53. Umar F, Hatta M, Husain DR, et al. Verapamil as an efflux inhibitor against drug resistant *Mycobacterium tuberculosis*: a review. *Syst Rev Pharm.* 2019;10:S43-S48.
54. Heel RC, Brogden RN, Speight TM, Avery GS. Loperamide: a review of its pharmacological properties and therapeutic efficacy in diarrhoea. *Drugs.* 1978;15:33-52.
55. Amaral L, Martins M, Viveiros M, Molnar J, Kristiansen J. Promising therapy of XDR-TB/MDR-TB with Thioridazine an inhibitor of bacterial efflux pumps. *Curr Drug Targets.* 2008;9:816-819.
56. Machado D, Pires D, Perdigão J, et al. Ion channel blockers as antimicrobial agents, efflux inhibitors, and enhancers of macrophage killing activity against drug resistant *mycobacterium tuberculosis*. *PLoS One.* 2016;11:1-28.
57. Yamashita M. Auranofin: past to present, and repurposing. *Int Immunopharmacol.* 2021;101:108272.
58. Kim S, Thiessen PA, Bolton EE, et al. PubChem substance and compound databases. *Nucleic Acids Res.* 2016;44:1202-1213.
59. Boyle NMO, Banck M, James CA, Morley C, Vandermeersch T, Hutchison GR. Open Babel: an open chemical toolbox. *J Cheminf* 2011;3:1-14.
60. Daina A, Michielin O, Zoete V. SwissADME: a free web tool to evaluate pharmacokinetics, drug-likeness and medicinal chemistry friendliness of small molecules. *Nat Publ Gr.* 2017;7:1-13.
61. Banerjee P, Kemmler E, Dunkel M, Preissner R. ProTox 3.0: a webserver for the prediction of toxicity of chemicals. *Nucleic Acids Res.* 2024;52:513-520.
62. Cheng F, Li W, Zhou Y, et al. AdmetSAR: a comprehensive source and free tool for assessment of chemical ADMET properties. *J Chem Inf Model.* 2012;52:3099-3105.
63. Gál J, Szvetnik A, Schnell R, Kálmán M. The metD D-methionine transporter locus of *Escherichia coli* is an ABC transporter gene cluster. *J Bacteriol.* 2002;184:4930-4932.
64. Mattar S, Scharf B, Kent SB, Rodewald K, Oesterheld D, Engelhard M. The primary structure of halocyanin, an archaeal blue copper protein, predicts a lipid anchor for membrane fixation. *J Biol Chem.* 1994;269:14939-14945.
65. Hayashi S, Wu C. Mini-review lipoproteins in bacteria. *J Bioenerg Biomembr.* 1990;22:451-471.
66. Klein P, Somorjai RL, Lau PC. Distinctive properties of signal sequences from bacterial lipoproteins. *Protein Eng.* 1988;2:15-20.
67. Sarkar T, Bharadwaj KK, Salauddin M, Pati S, Chakraborty R. Phytochemical characterization, antioxidant, anti-inflammatory, anti-diabetic properties, molecular docking, pharmacokinetic profiling, and network pharmacology analysis of the major phytoconstituents of raw and differently dried *Mangifera indica* (Himsagar cultivar): an in vitro and in silico investigations. *Appl Biochem Biotechnol.* 2022;1:1-38.
68. Chakma V, Barman DN, Das SC, et al. In silico analysis of a novel hypothetical protein (YP\_498675.1) from *Staphylococcus aureus* unravels the protein of tryptophan synthase beta superfamily (Try-synth-beta\_ II). *J Genet Eng Biotechnol.* 2023;21:135.
69. Naveed M, Makhdoom SI, Abbas G, et al. The virulent hypothetical proteins: the potential drug target involved in bacterial pathogenesis. *Mini-Reviews Med Chem.* 2022;22:2608-2623.
70. Jeba SH, Hasan MA, Faisal AS, et al. In silico approach of exploring the structural and functional characteristics of a hypothetical protein from monkeypox virus: a potential insight for antiviral therapeutics. *Microb Infect Dis.* Published Online 23 March 2024. doi:10.21608/mid.2024.272174.1818
71. Rabbi MF, Akter SA, Hasan MJ, Amin A. In silico characterization of a hypothetical protein from *Shigella dysenteriae* ATCC 12039 reveals a pathogenesis-related protein of the type-VI secretion system. *Bioinform Biol Insights.* 2021;15:11140.
72. Kwaik YA, Bumann D. Microreview microbial quest for food in vivo: 'nutritional virulence' as an emerging paradigm. *Cellular Microbiol.* 2013;15:882-890.
73. Sharaf NG, Shahgholi M, Kim E, et al. Characterization of the ABC methionine transporter from *Neisseria meningitidis* reveals that lipidated MetQ is required for interaction. *Elife.* 2021;10:1-21.
74. Soni DK, Dubey SK, Bhatnagar R. ATP-binding cassette (ABC) import systems of *Mycobacterium tuberculosis*: target for drug and vaccine development. *Emerg Microbes Infect.* 2020;9:207-220.
75. Naveed M, Imran K, Mushtaq A, Mumtaz AS, Janjua HA, Khalid N. In silico functional and tumor suppressor role of hypothetical protein PCNXL2 with regulation of the Notch signaling pathway. *RSC Adv.* 2018;8:21414-21430.
76. Hasan MA, Mazumder MHH, Chowdhury AS, Datta A, Khan MA. Molecular-docking study of malaria drug target enzyme transketolase in *Plasmodium falciparum* 3D7 portends the novel approach to its treatment. *Source Code Biol Med.* 2015;10:7.
77. Naveed M, Ali I, Aziz T, et al. Assessment of *Melia azedarach* plant extracts activity against hypothetical protein of *Mycobacterium tuberculosis* via GC-MS analysis and in silico approaches. *J Comput Biophys Chem.* 2024;23:299-320.
78. Wanek T, Römermann K, Mairinger S, et al. Factors governing P-Glycoprotein-mediated drug-drug interactions at the blood-brain barrier measured with positron emission tomography. *Mol Pharm.* 2015;12:3214-3225.
79. Leung K. [N-methyl-11C]4-(4-(4-Chlorophenyl)-4-hydroxypiperidin-1-yl)-2,2-diphenyl-N-dimethyl-butanamide. In: Leung K, ed. *Molecular Imaging and Contrast Agent Database.* National Center for Biotechnology Information; 2010.
80. van de Beek D, Brouwer M, Hasbun R, Koedel U, Whitney CG, Wijdicks E. Community-acquired bacterial meningitis. *Nat Rev Dis Prim.* 2016;2:16074.